

A nonlinear anisotropic model for porcine aortic heart valves

J. Li^a, X.Y. Luo^{b,*}, Z.B. Kuang^c

^a*School of Civil Engineering and Mechanics, Xi'an Jiaotong University, 710049 Xi'an, People's Republic of China*

^b*Department of Mechanical Engineering, The University of Sheffield, Sheffield S1 3JD, UK*

^c*School of Civil Engineering and Mechanics, Shanghai Jiaotong University, 200040 Shanghai, People's Republic of China*

Accepted 30 May 2001

Abstract

The anisotropic property of porcine aortic valve leaflet has potentially significant effects on its mechanical behaviour and the failure mechanisms. However, due to its complex nature, testing and modelling the anisotropic porcine aortic valves remains a continuing challenge to date. This study has developed a nonlinear anisotropic finite element model for porcine heart valves. The model is based on the uniaxial experimental data of porcine aortic heart valve leaflet and the properties of nonlinear composite material. A finite element code is developed to solve this problem using the 8-node super-parameter nonlinear shells and the update Lagrangian method. The stress distribution and deformation of the porcine aortic valves with either uniform and non-uniform thicknesses in closed phase and loaded condition are calculated. The results showed significant changes in the stress distributions due to the anisotropic property of the leaflets. Compared with the isotropic valve at the same loading condition, it is found that the site of the peak stress of the anisotropic leaflet is different; the maximum longitudinal normal stress is increased, but the maximum transversal normal stress and in-plane shear stress are reduced. We conclude that it is very important to consider the anisotropic property of the porcine heart valves in order to understand the failure mechanism of such valves in vivo. © 2001 Elsevier Science Ltd. All rights reserved.

Keywords: Bioprosthetic heart valve; Anisotropic; Stress analysis; Finite element methods

1. Introduction

The use of prosthetic heart valves in replacing diseased natural valves has become a routine procedure in the last 50 years. There are two basic types of prosthetic valves: mechanical ones and bioprosthetic ones. Compared to the mechanical valves, bioprosthetic heart valves also have successful performance and there is no need for the patient to have immunosuppressive therapy, but their long-term performance has been disappointing. Most of the degeneration of bioprosthetic heart valves can be attributed to calcification and tearing of leaflets. The stress concentration is thought to be one of the main reasons responsible for the degeneration.

Numerical simulation of bioprosthetic heart valve has made significant contributions to analysis of the stress distributions and design optimizations of bioprosthetic heart valves. Some of these studies used the linear isotropic models for the valves (Gould et al., 1973; Ghista and Reul, 1977), others used nonlinear isotropic

models (Hamid et al., 1985, 1986; Huang et al., 1990; Black et al., 1991; Krucinski et al., 1993; Thornton et al., 1997). It was found that the stress of leaflet is sensitive to geometrical variations of the leaflets (Gould et al., 1973), and that a proper design of the supporting stent can significantly reduce the flexural stresses (Krucinski et al., 1993). Patterson et al. (1996) presented a study of linear and nonlinear isotropic elastic model of the leaflets during the cardiac cycle, they found that the nonlinear model was more responsive to time-varying pressure wave, and induces lower compressive but higher tensile stresses in the leaflets. Christie and Medland (1982) and Christie and Barrattboyes (1991) used membrane and truss elements to simulate anisotropic behaviour of bioprosthetic heart valves. They found significant stress reductions at the commissures due to the anisotropy. Rousseau et al. (1988) also simulated the heart valve with linear anisotropic viscoelastic behaviour using membrane and truss elements. Grande et al. (1998, 1999) used the ANSYS software to analyse the aortic valve with linear anisotropic behaviour. Hart et al. (1998) used the MARC software to simulate the fibre-reinforced synthetic aortic

*Corresponding author.

E-mail address: x.y.luo@sheffield.ac.uk (X.Y. Luo).

valve prosthesis and found that in peak stress areas of reinforced models, up to 60% of the maximum principal stresses is taken over by fibres. Recently, the anisotropic behaviour (orthotropy) of a pericardium heart valve has been analysed by Burriesci et al. (1999) using a commercial package LS DYNA and they have found that even a small amount of orthotropy can significantly affect the mechanical behaviour of the valve.

Most of the above studies, however, have oversimplified or overlooked the nonlinear anisotropic property of the valve material. This is especially true when native porcine aortic valve leaflets are used. The porcine valve leaflets can be regarded as an elastic meshwork, reinforced with stiff collagen bundles, showing an arrangement in one particular direction (Sauren et al., 1980). Several uniaxial (Broom, 1977; Rousseau et al., 1983; Sauren et al., 1983; Mavrilas and Missirlis, 1991; Vesely and Noseworthy, 1992; Vesely and Lozon, 1993; Purinya and Kasyanov, 1994; and Vesely et al., 1995) and a very few biaxial (Mayne et al., 1989; Billiar and Sacks, 2000) studies have been conducted on porcine aortic valve leaflets. These studies showed that the circumferential elastic modulus of porcine aortic valve leaflet is about 6 times as large as the radial elastic modulus (and the difference is even greater in human aortic heart valves). The reason is due to the particular microstructure of the heart valve leaflet, because the collagen fibres in the valve leaflets are mainly oriented in the circumferential direction. Therefore, porcine heart valves can be seen as a fibre-reinforced composite, see Fig. 1. To the best knowledge of the authors, work has not been done to treat the porcine valve as a composite shell material where the nonlinear anisotropy can be considered properly according to experimental observations.

In this paper, a nonlinear anisotropic model for porcine heart valves is developed based on the uniaxial experimental study of Mavrilas and Missirlis (1991) and transversely isotropic composite material model. The finite element method is used to calculate the stress distribution of the valve leaflet using the update Lagrangian method and 8-node nonlinear shell elements. Results are compared with corresponding isotropic and linear models. The effect of non-uniform thickness is also assessed.

The constitutive model is developed in Section 2, the finite element method is presented in Section 3, followed by the finite element model of the porcine valve in Section 4. The results are shown in Section 5. Finally, discussion and conclusion are given in Section 6.

2. The constitutive model for the porcine heart valve leaflet

The leaflets of porcine aortic valve are reinforced with collagen and elastin fibres, and behave like the

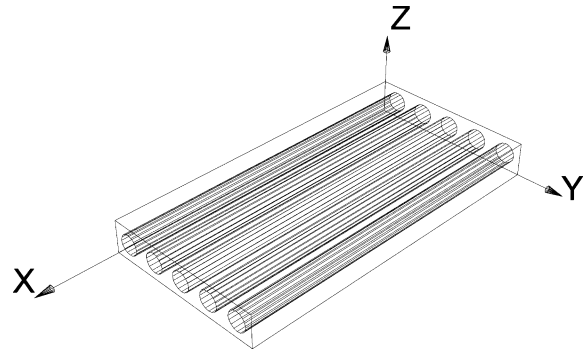


Fig. 1. A fibre-reinforced composite material model.

anisotropic fibre-reinforced composite. Fibre-reinforced structure is a simple composite with transverse isotropy, see Fig. 1, where X is the longitudinal direction of fibre. The mechanical behaviour of the structure is the same in Y and Z directions.

A transversely isotropic material has five elastic moduli, namely, E_x , E_y , ν_{xy} , ν_{yz} and G_{xy} , where E_x , E_y are the Young's moduli in longitudinal direction X , and transverse direction Y , respectively, ν_{xy} , ν_{yz} are the Poisson's ratios of XY plane and YZ plane, respectively, and G_{xy} is the shear modulus of the XY plane.

The nonlinear stress–strain relations for the transversely isotropic material can be written in matrix form as

$$\{\sigma\} = [D_A(E)]\{\varepsilon\}, \quad (1)$$

where $[D_A(E)]$ is the stiffness matrix of the transversely isotropic composite depends on Young's moduli, E . The Young's moduli can be determined from the porcine valve experiments. Although there are few biaxial experiments for the porcine aortic heart valves in literature (Mayne et al., 1989; Billiar and Sacks, 2000), the data published are incomplete. Hence as a first step, a well-established uniaxial experiment by Mavrilas and Missirlis (1991) for porcine aortic heart valves is used in this paper. For a typical stress–strain curve of soft tissues in an uniaxial experiment, the nonlinear elastic module $E(\varepsilon)$ is a function of strain:

$$E(\varepsilon) = \frac{d\sigma(\varepsilon)}{d\varepsilon}. \quad (2)$$

To extend this in three dimensions, the incremental stress–strain constitutive equation can be written as

$$\{\Delta\sigma\} = [D_A(E(\bar{\varepsilon}))]\{\Delta\varepsilon\}, \quad (3)$$

where $\bar{\varepsilon}$ is the effective strain, defined as

$$\bar{\varepsilon} = \frac{\sqrt{(\varepsilon_x - \varepsilon_y)^2 + (\varepsilon_y - \varepsilon_z)^2 + (\varepsilon_z - \varepsilon_x)^2 + \frac{3}{2}(\gamma_{xy}^2 + \gamma_{yz}^2 + \gamma_{zx}^2)}}{\sqrt{2(1 + \nu)}}$$

In order to determine the moduli E_x and E_y , and G_{xy} using the uniaxial experimental data (Mavrilas and

Missirlis, 1991), we assume that both the fibre and the matrix are isotropic materials with the same Poisson ratio. As the soft tissue is incompressible, a uniform Poisson's ratio is used:

$$v_{xy} = v_{yz} = 0.45. \quad (4)$$

Using the law of mixtures formula (Garg et al., 1973), we have

$$E_x = E_f V_f + E_m V_m, \quad 1/E_y = V_f/E_f + V_m/E_m, \quad (5)$$

$$v_{xy} = v_f V_f + v_m V_m, \quad 1/G_{xy} = V_f/G_f + V_m/G_m, \quad (6)$$

where V_f , V_m are the proportional volumes of the fibre and the matrix material, respectively. In this study, we assume $V_f = V_m = 0.5$ (Vesely and Noseworthy, 1992). The moduli with the suffix f and m indicate the property of the fibre and the matrix material, respectively, while the suffix x and y indicate the property of the fibre-reinforced composite in longitudinal and transversal directions, respectively. As E_x is much greater than E_y , it can be derived straightforwardly that $G_{xy} = E_y/[2 \times (1 + v_{xy})]$.

Again, in order to use the uniaxial experimental data, we assume that the coupling effects of strains on x, y directions are small, i.e., the following relations hold:

$$E_x = E_x(\epsilon_x), \quad E_y = E_y(\bar{\epsilon}). \quad (7)$$

This then allows us to interpolate the experimental data by Mavrilas and Missirlis (1991) in Fig. 2 using the following expressions:

$$E_x = 1927.2e^{9.827\epsilon_x} \text{ (kPa)},$$

$$E_y = 118.34e^{13.20\bar{\epsilon}} \text{ (kPa)}. \quad (8)$$

3. The finite element model

3.1. The finite element method

Because the leaflets of porcine aortic heart valve are thin and soft, Reissner–Mindlin assumptions (Zienkiewicz, 1998) and the 8-node shell elements are used. To define the essential strains and stresses we choose the local orthogonal axes (x' , y' , z') on the surface $\zeta = \text{constant}$, where z' is normal to the surface, x' , y' are in the $\xi\eta$ plane. Let \vec{V}_1 , \vec{V}_2 and \vec{V}_3 be the unit vectors of the local orthogonal axes and $\vec{\xi}$ and $\vec{\eta}$ denote the two unit vectors tangent to ξ and η ($\zeta = \text{constant}$), the curvilinear coordinates in the middle plane of the shell. To deal with the fibre-reinforced material, we need to track the material principle direction (longitudinal direction of fibre) during the total load phases. In this paper, we divided the elements in such a way so that η is along the longitudinal direction of fibre.

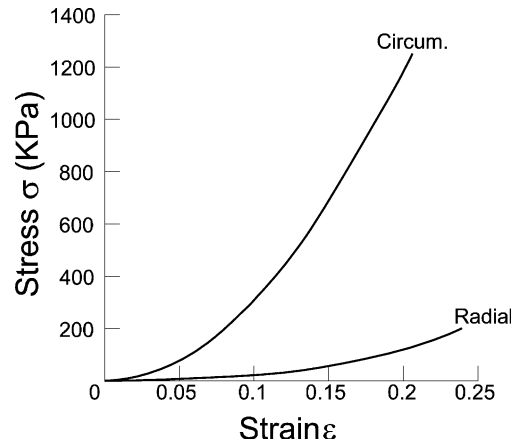


Fig. 2. Stress–strain diagrams of porcine aortic in the circumferential and radial directions.

Apply the principle of virtual work and boundary conditions to Eq. (2) and drop the small higher order terms, we can write the global matrix equation as

$${}^t[K]{}^{t+\Delta t}\{U\} = {}^{t+\Delta t}\{R\} - {}^{t+\Delta t}\{F\}, \quad (9)$$

where $[K]$ is the stiffness matrix, $\{U\}$ is the displacement vector, $\{R\}$ is the load vector and $\{F\}$ is the force residual vector. This nonlinear problem is solved incrementally using the update Lagrangian method. During each step, a linear algebraic equation is solved using the modified Newton–Raphson method.

3.2. The geometry of the porcine valve

The shape of porcine aortic heart valve leaflet in closed and unloaded phase is assumed to be an elliptic paraboloid (Hamid et al., 1986), see Fig. 3. Following Hamid et al. (1986), we chose the inner diameter of the valve to be 27.8 mm, a stent height to be 19 mm and a surface area to be 5.77 cm². The finite element mesh is shown for a whole leaflet in Fig. 4. However, we assume that the three leaflets are identical and that each one is symmetric about its own midline, hence only half of a leaflet is calculated. The element number in the computation is 900, with 2821 nodes.

3.3. Boundary conditions

We assume that the leaflet is firmly attached to the stent (line BC) and the stent is rigid, so that displacements are zero but rotations are allowed on this boundary. Due to the symmetry, the displacement and the angle of the normal line of leaflet around the midline AC are set to zero, $u = 0, \beta = 0$.

The free edge AB contacts with its neighbouring leaflets, hence all the nodes on AB cannot move across the plane $\theta = 60^\circ$, but can move along axis Z . For the

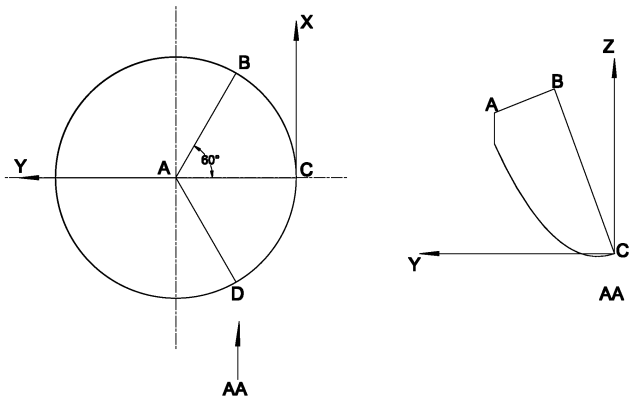


Fig. 3. The geometry model of the porcine aortic heart valve. Left is the view from the top of the heart valve, right is the side view. BAD is the free edge; A is the centre point of the free edge; BCD is the commissure edge; AC is the middle line of the leaflet.

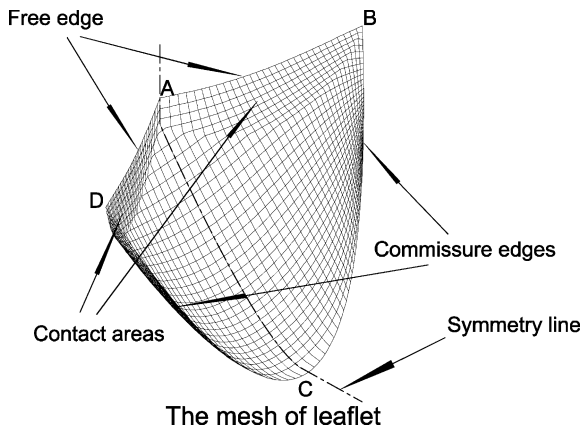


Fig. 4. The finite element mesh of the total leaflet.

nodes that already reached the plane $\theta = 60^\circ$, the incline restraint condition is imposed: $u = v/\tan 60^\circ$. The contact forces of the nodes on the plane $\theta = 60^\circ$ are checked in every increment. If the contact force of a node is tensile, the node will be released and if the contact force is compressive, the node remains in contact. This ensures that the contact is not ‘adhesive’.

3.4. Incremental pressure loading

An uniform systolic pressure of $P = 16 \text{ kPa}$ (120 mm Hg) is assumed on the outflow surface (top-surface) of leaflet, and pressure free is assumed on the inflow surface (bottom-surface). To achieve the convergence, an incremental pressure loading is used in the simulation. Following the change of the nonlinear Young’s modulus (8), the increment of pressure at the n th step is chosen as

$$\Delta P_n = P_0 e^{c(n-1)}, \tag{10}$$

where P_0 is the starting pressure, taken to be 0.7 kPa here, and c is a constant, $c = 0.04$.

3.5. Code validations

The finite element code has been validated in four different ways. First, a bench-mark comparison is made with work by Surana (1983) and Sabir and Lock (1973), where the nonlinear isotropic cylindrical shell with concentrated load was analysed. The load–deflection curve of the cylindrical shell obtained from our code is in excellent agreement with the results of Surana (1983) and Sabir and Lock (1973), see Fig. 5.

Secondly, the first principal stress distribution for isotropic valve is compared with the one from Hamid et al. (1986), where the membrane model is used. It is found that although there are small differences in the location and value of the peak stress due to the different Young’s modulus and mechanical models used, the qualitative feature of the stress distributions are similar in both cases.

It is difficult to find the published result for nonlinear and anisotropic shells. Hence, we verified our code by simulating the uniaxial stretch along the longitudinal and transversal directions, respectively. The calculated results also present similar uniaxial stretches as it should be. Thus, the transverse property of the model is represented correctly by our code.

Finally, different number of the elements and incremental loading steps are used to check if the results are element and incremental step independent, and to obtain the best economical choice. There is always a delicate balance between making the element small

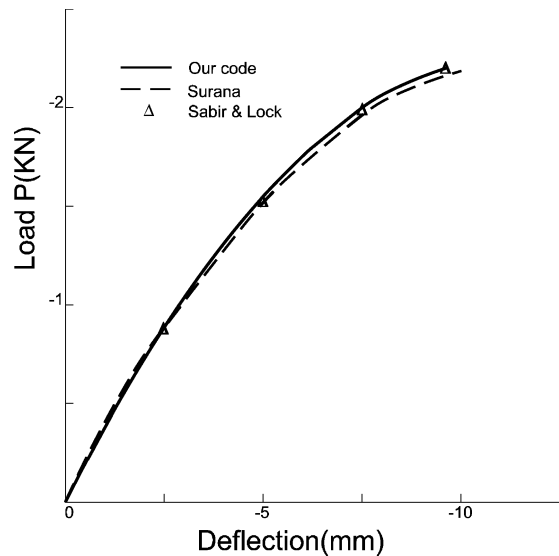


Fig. 5. Comparison of load–deflection curves for a cylindrical shell ($h = 12.7 \text{ mm}$) with the ones by Surana (1983) and Sabir and Lock (1973).

enough to obtain accurate results and yet large enough to reduce the computational efforts. It is found that the results of 30×30 (900 elements) and 40×40 (1600 elements) are almost identical. Also, the results become independent to incremental steps for loading over 60 increments. Hence, the mesh with 900 elements and 60 incremental steps are chosen to analyse the half leaflet.

4. Results

The stress distributions of the nonlinear anisotropic valves are calculated. In the following, the effects of the isotropy, the nonlinearity, and non-uniform thickness of the porcine valve leaflets are presented. Usually, the first principal stresses and maximum shear stresses are used to analyse the stress distributions for isotropic material, but for anisotropic material, it makes more sense to discuss the longitudinal normal stresses, transversal stresses and shear stresses. Hence, in order to compare the results of isotropic leaflets with the anisotropic one, both types of stresses may be shown here.

4.1. The effects of anisotropy with uniform thickness

Fig. 6 shows the fibre directions over the anisotropic leaflet surface. The leaflet has a uniform thickness of 0.6 mm (Hamid et al., 1986). Stress distribution is calculated both for the anisotropic and isotropic leaflets. The Young's modulus for the isotropic leaflet is assumed to be half of the circumferential Young's modulus of anisotropic leaflet.

Fig. 7 shows the contours of the first principal stress over the leaflet surface for isotropic (left half) and anisotropic leaflet (right half). The view is as the leaflet would appear if it was removed from the stent and laid out flat; the free (or coapting) edge is the line DAB and the line DCB is the suture line at the stent frame. It is seen that the stress distribution of anisotropic leaflet is quite different from the isotropic one. First of all, the site of peak stress of isotropic leaflet is found to be located at the stent apex (D); while the anisotropic peak stress is located on the commissure edge, much lower than the isotropic one. The maximum peak stress is much higher in the anisotropic case, but this is understandable, since the anisotropic leaflet has higher Young's modulus in the longitudinal normal direction. This can be seen more clearly in Fig. 8, where the contours of the longitudinal normal stresses, transversal normal stresses and in-plane shear stresses are given. Although the maximum longitudinal normal stresses of anisotropic leaflet is greater than isotropic one, the maximum transversal normal stresses and shear stress of anisotropic leaflet are greatly reduced.

The deformation of the isotropic and anisotropic leaflets is also different, as shown in Fig. 9. It is clear

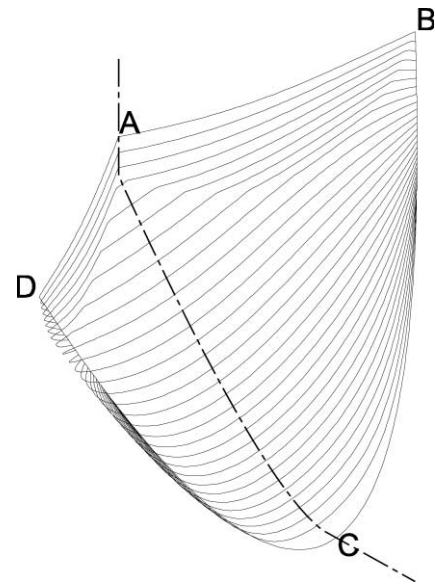


Fig. 6. The fibre arrangement of the leaflet.

that the deformation of the symmetry line AC is greater in anisotropic leaflet. This is because that the stiffness in the axial direction is reduced by the anisotropy.

The effective bending moment per unit length is calculated from the top and surface planes from $M = \sqrt{(M_x^2 + M_y^2 - M_x M_y + 3M_{xy}^2)}$, where $M_x = (\sigma_x^{\text{top}} - \sigma_x^{\text{bottom}})h^2/12$, $M_y = (\sigma_y^{\text{top}} - \sigma_y^{\text{bottom}})h^2/12$ and $M_{xy} = (\tau_{xy}^{\text{top}} - \tau_{xy}^{\text{bottom}})h^2/12$. Contours of the bending moment for both leaflets are given in Fig. 10. We noted that the maximum bending moment occurs at the location of the coapting area where the leaflet contacts with another one. Although not plotted, we found the maximum compressive stress also occurs there. This is true for both anisotropic and isotropic cases. The principal difference between the anisotropic and isotropic ones is that the former tends to reduce the peak values of the bending moment and compressive stress.

4.2. The effects of the nonlinearity

The longitudinal normal stress distribution of the nonlinear anisotropic leaflet with a uniform thickness of 0.6 mm is shown in Fig. 11. The results are compared with the stress contours from the corresponding linear anisotropic leaflet. Three different values of the Young's modulus (low $E_x = 2483$ kPa, middle $E_x = 3172$ kPa and high $E_x = 5793$ kPa; $E_x/E_y = 6$) is used for the linear leaflet. It is clear that the maximum stress of the linear valves increases with the increase of E_x . However, the site of the peak stress is the same for the linear leaflets for all different values of E_x . This is different to the nonlinear case, where the site of the peak stress is moved up, albeit slightly, towards the stent. The contours of the stress of the nonlinear leaflet near the

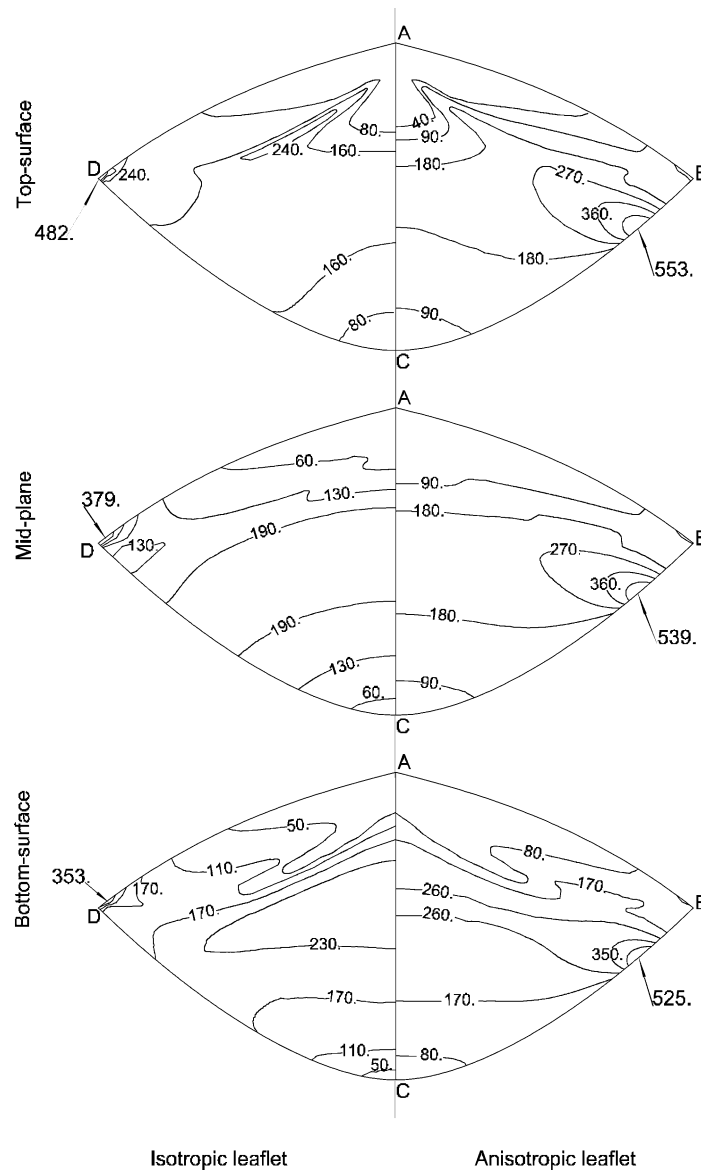


Fig. 7. The first principal stress distribution of isotropic (left) and anisotropic (right) leaflets. The values on the contours are given in kPa.

site of the peak stress also seem to be narrower than the linear ones.

4.3. The effects of the non-uniform thickness

The thickness of the porcine heart valve leaflet is non-uniform (Clark and Finke, 1974). The pattern of the stress distribution can be strongly influenced by the thickness variation of the leaflet. This is investigated by varying the thickness of the anisotropic leaflet from 0.2 to 1.4 mm, where the thicknesses of A–C are taken from the measured data by Clark and Finke (1974). The internal distribution is assumed to be parabolic, see Fig. 12. Results of both isotropic and anisotropic leaflet with non-uniform thickness is shown in Fig. 13. This should

be compared with Fig. 7. For both cases, the stress distribution of the non-uniform leaflet seems to be more homogeneous due to the non-uniform thickness. For isotropic case, the site of the maximum principal stress remains the same, at point D. However, there is a secondary maximum principal stress located at the belly of the valve when the thickness of the valve is non-uniform. This phenomenon is even more pronounced in the anisotropic case, where the peak principal stress actually locates in the belly zone, and the stress at the commissures is reduced by 43%, see Fig. 7. This is in agreement with the pathological examination of excised valves by Carpentier et al. (1976) that the leaflet's belly zone to be a common site of tissue rupture and disruption. There are two major differences between

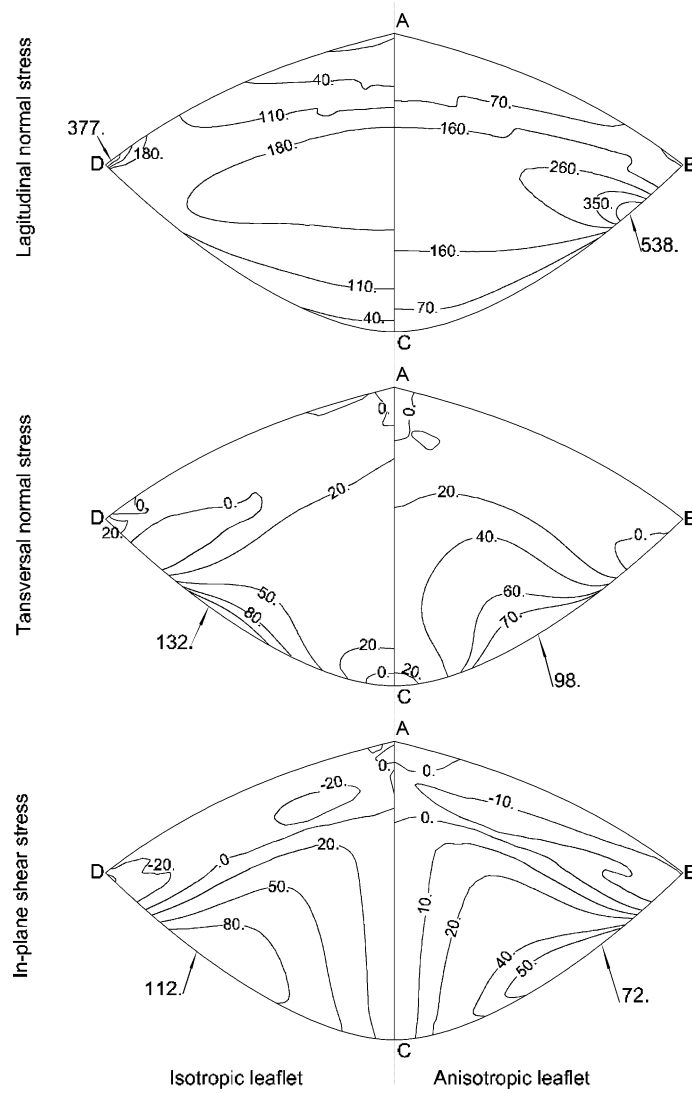


Fig. 8. The longitudinal normal stress (top-figures), transverse normal stress (middle-figures) distribution of isotropic (left-figures) and anisotropic (right-figures) leaflets. The values on the contours are given in kPa.

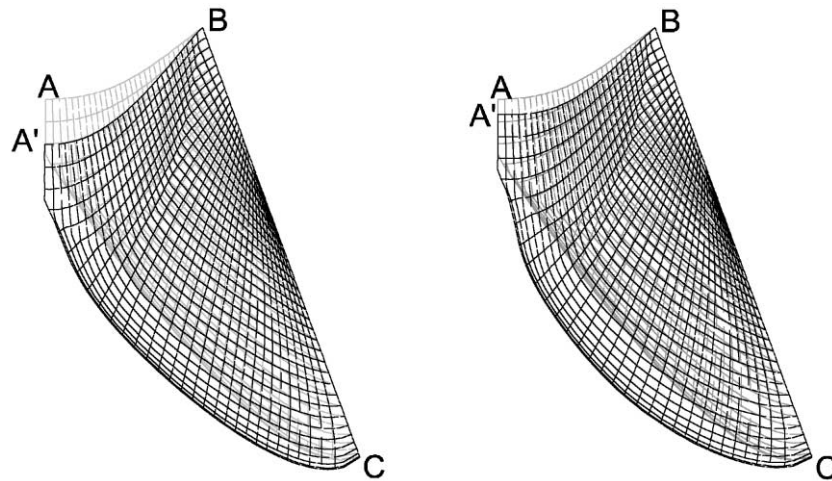


Fig. 9. The deformations of isotropic (left) and anisotropic (right) leaflets.

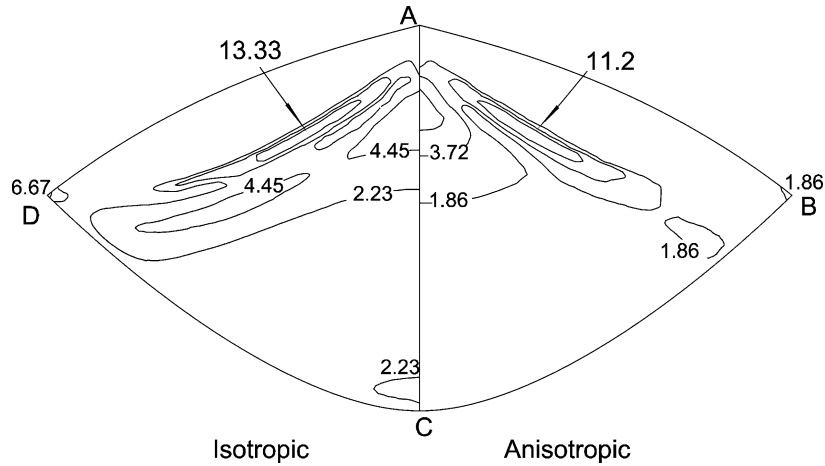


Fig. 10. The distribution of bending moment per unit length of isotropic (left) and anisotropic (right) leaflets. The values on the contours are given in $10^{-3} \text{ N mm mm}^{-1}$.

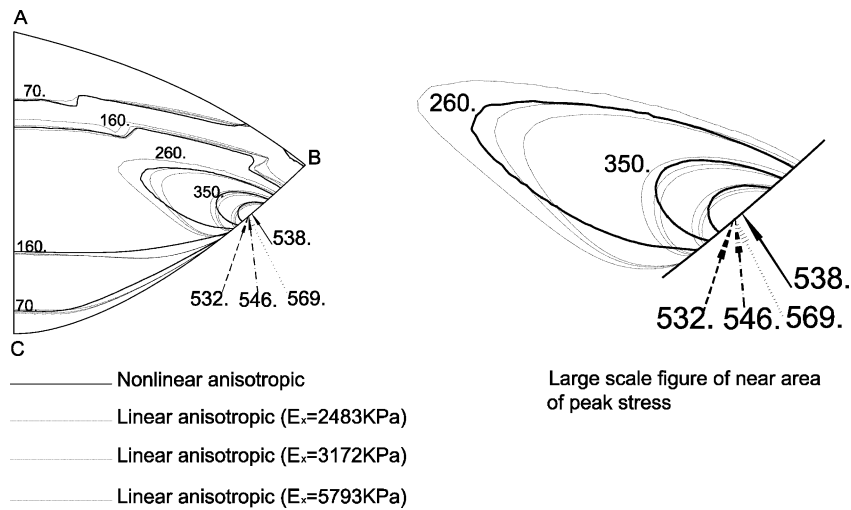


Fig. 11. The longitudinal normal stress of mid-plane of linear and nonlinear analysis of leaflet. A larger scale of the peak stress area is shown on the right. The values on the contours are given in kPa.

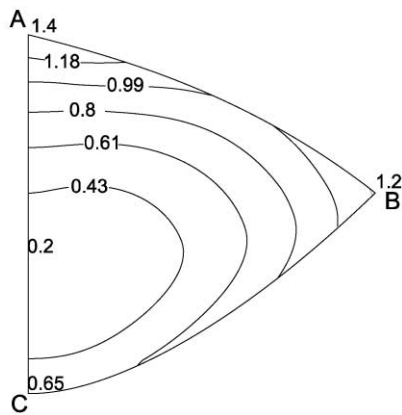


Fig. 12. The thickness distribution of non-uniform thickness leaflet. The values on the contours are given in mm.

the isotropic and anisotropic ones with non-uniform thickness. One is that the site peak stress, one locates at point D, the other locates at the belly zone; the second one is the higher stress level along the commissures for the anisotropic valve.

5. Discussion and conclusion

The nonlinear anisotropic finite element computational model is developed to analyse the porcine aortic heart valve. The influences of the anisotropy, non-linearity, and the non-uniform thickness of the valve leaflets are analysed, respectively. Our results showed significant changes in the stress patterns due to

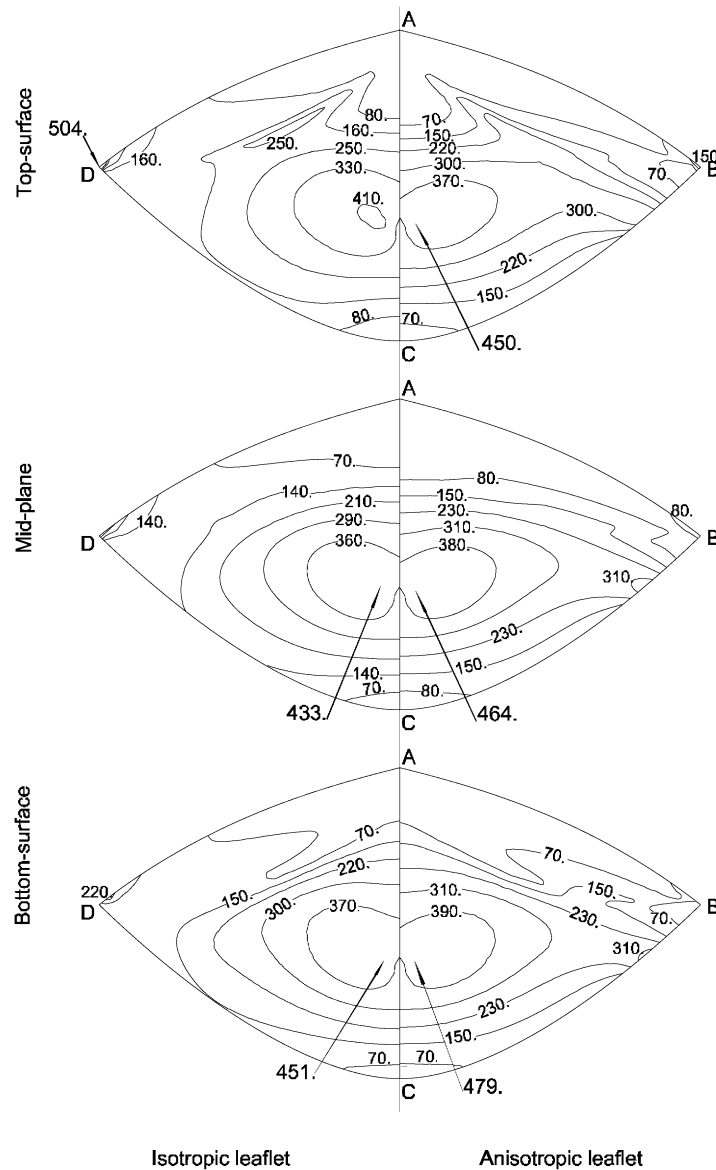


Fig. 13. The first principal stress distributions of isotropic (left) and anisotropic (right) leaflets with non-uniform thickness. The values on the contours are given in kPa.

the nonlinear anisotropic behaviour of the porcine valves.

For valves with uniform thickness, it is found that the anisotropic valve gives rise to much smaller shear and transversal normal stresses, but greater longitudinal normal stress located near the commissures just below the attachment point D. The greater longitudinal normal stress shows that much of the load is carried along the longitudinal or fibre direction.

The fact that we found the anisotropy of the valves enhances the stress concentration at the commissures initially seems to be contradictory to the main conclusion made by Christie and Medland (1982) using a membrane model. However, this can be explained by

the fact that their results are presented as membrane stress only, which is separated from the stress sheared by the fibre elements. We calculated the whole stress of the composite material, therefore the stress concentration should be higher in the area where the material is more reinforced.

We found that the bending moment and the compressive stress are located primarily at the contact area of the leaflet, although the stress level is reduced by the anisotropic property. This is different from the observations by Burriesci et al. (1999) where they found the maximum bending and compressive stresses are near the commissures. This is because the forces in their time-dependent model are transmitted from the stent when

the valves are moving dynamically. In our static model, the contact area experiences the largest bending force and compressions.

Introducing the nonlinearity in the valves makes two changes in the longitudinal normal stress distribution. Compare with the linear valves, it changes the location of the peak stress, therefore, the possible failure site (if the failure is directly associated with the static peak stress); it also changes the distribution of stress pattern. However, it should be stated that the changes caused by the nonlinearity are small here, presumably because we only considered static valves. Non-uniform thickness of the valve tends to even the stress distribution in both isotropic and anisotropic cases. This is perhaps the reason why the nature valves choose to be non-uniform. The site of the peak stress for the anisotropic valve is located at the belly zone, while for the isotropic valve it appears at the attachment point D.

It should be pointed out that our anisotropic model is based on an uniaxial experiment where only two of the five Young's moduli can be determined. It would be greatly improved if all five Young's moduli can be obtained from experiments directly so that approximations in deriving v_x , v_y , and G_{xy} are no longer needed. Nevertheless, as a first step, this model has provided us with some new understandings of influences that the nonlinear anisotropy may have on the mechanical behaviour of the porcine heart valves.

Acknowledgements

We gratefully acknowledge the Royal Society for providing the first author a China fellowship to carry out this research project in the UK.

References

- Billiar, K.L., Sacks, M.S., 2000. Biaxial mechanical properties of the native and glutaraldehyde-treated aortic valve cusp: Part I—experimental results. *Journal of Biomechanical Engineering, ASME* 122, 23–30.
- Black, M.M., Howard, I.C., Huang, X., Patterson, E.A., 1991. Three-dimensional finite element analysis of a bioprosthetic heart valve. *Journal of Biomechanics* 24, 793–801.
- Broom, N.D., 1977. The stress/strain and fatigue behaviour of glutaraldehyde preserved heart-valve tissue. *Journal of Biomechanics* 10, 707–724.
- Burriesci, G., Howard, I.C., Patterson, E.A., 1999. The stress/strain and fatigue behaviour of glutaraldehyde preserved heart-valve tissue. *Journal of Biomechanics* 10, 707–724.
- Carpentier, A., Deloche, A., Relland, J., Dubost, C., 1976. Valvular xenograft and valvular bioprosthesis: 1965–1975. In: Kalmanson, D. (Ed.), *The Mitral Valves: A Pluridisciplinary Approach*. Edward Arnold, London, pp. 505–518.
- Christie, G.W., Medland, I.C., 1982. A non-linear finite element stress analysis of bioprosthetic heart valves. In: Gallagher, R.H., et al. (Eds.), *Finite Elements in Biomechanics*. Wiley, Chichester, pp. 153–179.
- Christie, G.W., Barrattboyes, B.G., 1991. On stress reduction in bioprosthetic heart-valve leaflets by the use of a flexible. *Journal of Cardiac Surgery* 6, 476–481.
- Clark, R.E., Finke, E.H., 1974. Scanning and light microscopy of human aortic leaflets in stressed and relaxed stress. *Journal of Cardiovascular Surgery* 67 (5), 792–803.
- Garg, S.K., Svalbonas, V., Gurtman, G.A., 1973. *Analysis of Structural Composite Materials*. Marcel Dekker, Inc, New York.
- Ghista, D.N., Reul, H., 1977. Optimal prosthetic aortic leaflet valve: design parametric and longevity analyses: development of the Avcothane-51 leaflet valve based on the optimum design analysis. *Journal of Biomechanics* 10, 313–324.
- Gould, P.L., Cataloglu, A., et al., 1973. Stress analysis of the human aortic valve. *Computers and Structures* 3, 377–384.
- Grande, K.J., Cochran, R.P., Reinhall, P.G., Kunzelman, K.S., 1998. Stress variations in the human aortic root and valve: the role of anatomic asymmetry. *Annals of Biomedical Engineering* 26, 534–545.
- Grande, K.J., Cochran, R.P., Reinhall, P.G., Kunzelman, K.S., 1999. Mechanisms of aortic valve incompetence in aging: a finite element model. *Journal of Heart Valve Disease* 8, 149–159.
- Hamid, M.S., Sabbah, H.N., Stein, P.D., 1985. Finite element evaluation of stresses on closed leaflets of bioprosthetic heart valves with flexible stents. *Finite Elements in Analysis and Design* 1, 213–225.
- Hamid, M.S., Sabbah, H.N., Stein, P.D., 1986. Influence of stent height upon stresses on the cusps of closed bioprosthetic valves. *Journal of Biomechanics* 19, 759–769.
- Hart, J., Cacciola, G., Schreurs, P.J.G., Peters, G.W.M., 1998. A three-dimensional analysis of a fibre-reinforced aortic valve prosthesis. *Journal of Biomechanics* 31, 629–638.
- Huang, X., Black, M.M., Howard, I.C., Patterson, E.A., 1990. Two-dimensional finite element analysis of a bioprosthetic heart valve. *Journal of Biomechanics* 23, 753–762.
- Krucinski, S., Vesely, I., Dokainish, M.A., et al., 1993. Numerical simulation of leaflet flexure in bioprosthetic valves mounted on rigid and expansible stents. *Journal of Biomechanics* 26, 929–943.
- Mayne, A.S.D., Christie, G.M., Smail, B.H., Hunter, P.J., Barratt-Boyes, B.G., 1989. An assessment of the mechanical properties of leaflets from four second-generation porcine bioprostheses with biaxial testing techniques. *Journal of Thoracic Cardiovascular Surgery* 98, 170–180.
- Mavrilas, D., Missirlis, Y., 1991. An approach to the optimisation of preparation of bioprosthetic heart valves. *Journal of Biomechanics* 24, 331–339.
- Patterson, E.A., Howard, I.C., Thornton, M.A., 1996. A comparative study of linear and nonlinear simulations of the leaflets in a bioprosthetic heart valve during the cardiac cycle. *Journal of Medical Engineering and Technology* 20, 95–108.
- Purinya, B., Kasyanov, V., 1994. Biomechanical and structural properties of the explanted bioprosthetic valve leaflets. *Journal of Biomechanics* 27, 1–11.
- Rousseau, E.P.M., Sauren, A.A.H.J., Hout, M.C.Van, Steenhoven, A.A.Van, 1983. Elastic and viscoelastic material behaviour of fresh and glutaraldehyde-treated porcine aortic valve tissue. *Journal of Biomechanics* 16, 339–348.
- Rousseau, E.P.M., Steenhoven, A.A.Van, Janssen, J.D., 1988. A mechanical analysis of the closed Hancock heart valve prosthesis. *Journal of Biomechanics* 21, 545–562.
- Sabir, A.B., Lock, A.C., 1973. The application of the finite elements to the large deflection geometrically non linear behaviour of cylindrical shells. In: Brebia, C.A., Tottenham, H. (Eds.), *Variational Methods in Engineering*. Southampton University Press, 7/66–7/75.

- Surana, K.S., 1983. Geometrically nonlinear formulations for the curved shell elements. *International Journal of Numerical Methods in Engineering* 19, 581–615.
- Sauren, A.A.H.J., Kuijpers, W., Steenhoven, A.A., Veldpaus, F.E., 1980. Aortic valve histology and its relation with mechanics—preliminary report. *Journal of Biomechanics* 13, 97–104.
- Sauren, A.A.H.J., Hout, M.C.Van, Steenhoven, A.A.Van, Velspaus, F.E., Janssen, J.D., 1983. The mechanical properties of porcine aortic valve tissues. *Journal of Biomechanics* 16, 327–337.
- Thornton, M.A., Howard, L.C., Patterson, E.A., 1997. Three-dimensional stress analysis of polypropylene leaflets for prosthetic heart valves. *Medical Engineering and Physics* 19, 588–597.
- Vesely, I., Noseworthy, R., 1992. Micromechanics of the fibrosa and the ventricularis in aortic valve leaflets. *Journal of Biomechanics* 25, 101–113.
- Vesely, I., Lozon, A., 1993. Natural preload of aortic valve leaflet components during glutaraldehyde fixation: effects on tissue mechanics. *Journal of Biomechanics* 26, 121–123.
- Vesely, I., Boughner, D.R., Leesondietrich, J., 1995. Bioprosthetic valve tissue viscoelasticity—implications on accelerated pulse duplicator testing. *Annals of Thoracic Surgery* 60, S379–S383.
- Zienkiewicz, O.C., 1998. *The Finite Element Method*, 4th Ed. McGraw-Hill, London.